Journal of the Egyptian Mathematical Society (2016) **24**, 100–107

Egyptian Mathematical Society

Journal of the Egyptian Mathematical Society

www.etms-eg.org
www.elsevier.com/locate/joems

ORIGINAL ARTICLE

Thermal-diffusion and diffusion-thermo effects on MHD flow of viscous fluid between expanding or contracting rotating porous disks with viscous dissipation

S. Srinivas [a], **A. Subramanyam Reddy** [a,*], **T.R. Ramamohan** [b], **Anant Kant Shukla** [c]

[a] *Fluid Dynamics Division, School of Advanced Sciences, VIT University, Vellore 632014, India*
[b] *CSIR-CMMACS, Wind Tunnel Road, Bangalore 560 037, India*
[c] *Amrita School of Engineering, Amrita Vishwa Vidyapeetham, Amritanagar P.O., Coimbatore 641112, India*

Received 4 December 2013; revised 10 June 2014; accepted 18 June 2014
Available online 4 August 2014

KEYWORDS

Rotating porous disks;
Expansion ratio;
Dufour number;
Soret number;
Hartmann number;
Homotopy analysis method

Abstract The present work investigates the effects of thermal-diffusion and diffusion-thermo on MHD flow of viscous fluid between expanding or contracting rotating porous disks with viscous dissipation. The partial differential equations governing the flow problem under consideration have been transformed by a similarity transformation into a system of coupled nonlinear ordinary differential equations. An analytical approach, namely the homotopy analysis method is employed in order to obtain the solutions of the ordinary differential equations. The effects of various emerging parameters on flow variables have been discussed numerically and explained graphically. Comparison of the HAM solutions with the numerical solutions is performed.

MATHEMATICS SUBJECT CLASSIFICATION: 76D05; 80A20; 76W05

1. Introduction

The studies pertaining to laminar flow between parallel rotating disks have significant importance due to its applications in engineering and industry. Such type of applications can be found in semiconductor manufacturing process with rotating wafers, magnetic storage drives, gas turbine engines, electronic devices having rotary parts, and crystal growth process. The earliest work of steady flow over a disk of infinite rotating in an unbounded and quiescent fluid can be traced back to Von

* Corresponding author. Tel.: +91 416 2202514; fax: 0416 2243092.
E-mail address: anala.subramanyamreddy@gmail.com (A. Subramanyam Reddy).

Peer review under responsibility of Egyptian Mathematical Society.

ELSEVIER Production and hosting by Elsevier

1110-256X © 2014 Production and hosting by Elsevier B.V. on behalf of Egyptian Mathematical Society.
http://dx.doi.org/10.1016/j.joems.2014.06.017

Kármán [1]. Von Kármán [1] developed similarity transformations to analyze the steady flow of Newtonian fluid over rotating disk by transforming the Navier–Stokes equations into a system of coupled ordinary differential equations. The Numerical investigation of asymmetric flow of a micropolar fluid between porous disks has been explored by Ashraf et al. [2]. Kuiken [3] discussed the effects of normal blowing on the flow near the rotating disk of finite extent. Sparrow et al. [4] analyzed the flow about a porous-surfaced rotating disk. Nazir and Mahmood [5] analyzed flow and heat transfer of viscous fluid between contracting rotating disks. In their investigation they used Von Kármán similarity transformations to reduce the Navier–Stokes equations to system of ordinary differential equations and then resulting differential equations were solved by finite difference method. Their analysis showed that the velocity components and especially radial component of velocity have a strong influence on the temperature distribution inside the flow regime. Recently, Xinhui et al. [6] investigated the asymmetric laminar flow and heat transfer of viscous fluid between contracting rotating disks by the homotopy analysis method. The special boundary conditions and similarity transformations for the expanding or contracting walls were first proposed by Uchida and Aoki [7] in order to study the transport of biological fluids through expanding or contracting vessels, the synchronous pulsation of porous diaphragms, the air circulation in the respiratory system [6,8]. Majdalani and Zhou [9] studied moderate to large injection and suction driven channel flows with expanding or contracting walls. They used perturbations in the cross flow Reynolds number and the resulting equation was solved both numerically and asymptotically. Dauenhauer and Majdalani [10] studied the unsteady flow in semi-infinite expanding channels with wall injection. They proposed a procedure that leads to an exact similarity solution of Navier–Stokes equations in semi-infinite rectangular channels with porous and expanding walls. Recently, Xinhui et al. [11] studied the heat transfer in an asymmetric porous channel with expanding and contracting wall using HAM.

In many transport process in nature, flow is driven by density differences caused by temperature gradient, chemical composition (concentration) gradient and material composition. It is therefore important to study flow induced by concentration differences independently or simultaneously with temperature differences. The energy flux caused by the composition gradient is called the Dufour effect (diffusion-thermo). If the mass fluxes are created by temperature gradients, it is called the Soret effect (thermal-diffusion). These effects are generally of a small order of magnitude. The Soret effect plays an important role in the operation of solar ponds, biological systems, and the microstructure of the world oceans. In biological systems mass transport across biological membranes induced by small thermal gradients in living matter is an important factor. The Soret effect also is utilized for isotope separation and, in a mixture of gases of light molecular (H_2, He) and medium molecular weight (N_2, air). The Dufour effect was found to be of an order of magnitude such that it cannot be neglected [12]. Hayat et al. [13] studied thermal-diffusion and diffusion-thermo effects on axisymmetric flow of a second grade fluid by using homotopy analysis method. Osalusi et al. [14] examined numerically the effects of thermal-diffusion and diffusion thermo on combined heat and mass transfer of a steady hydromagnetic convective slip flow due to a rotating disk with viscous dissipation and ohmic heating. Recently, Srinivas et al. ([15] several references therein) studied the thermal diffusion and diffusion thermo effects in a two-dimensional viscous flow between slowly expanding or contracting walls with weak permeability.

From the extensive literature survey, it is noted that the problem of magnetohydrodynamic flow between parallel disks accounting thermal-diffusion and diffusion-thermo effects to the authors' knowledge has not yet been explored. Therefore, the objective of this investigation is to develop a mathematical model to understand the thermal-diffusion and diffusion-thermo on MHD flow of viscous fluid between expanding or contracting rotating porous disks with viscous dissipation. The governing equations in cylindrical coordinates are introduced and transformed into ordinary differential equations by using similarity transformations and then solved using a powerful technique recently developed by Liao [16] namely, the homotopy analysis method (HAM). It is worth to mention that HAM has been applied successfully to many interesting fluid flow problems [5,13,17–20]. The HAM solutions of the present investigation have been compared with the numerical solutions obtained by shooting method coupled with Runge–Kutta scheme and the results are found to be in excellent agreement.

2. Formulation of the problem

Consider laminar, incompressible flow of an electrically conducting viscous fluid between two parallel expanding or contracting rotating porous heated disks. The distance between the disks is $2a(t)$. Both disks are assumed to have different permeability and expand or contract uniformly at a time-dependent rate $\dot{a}(t)$. A magnetic field of uniform strength B_0 is applied perpendicular to the disks. As shown in Fig. 1, a cylindrical coordinate system may be chosen with the origin at the center between disks. Under these assumptions, the governing equations are given by [5,6]

$$\frac{1}{r}\frac{\partial(ru)}{\partial r}+\frac{1}{r}\frac{\partial v}{\partial \varphi}+\frac{\partial w}{\partial z}=0, \tag{1}$$

$$\frac{\partial u}{\partial t}+u\frac{\partial u}{\partial r}+\frac{1}{r}v\frac{\partial u}{\partial \varphi}+w\frac{\partial u}{\partial z}-\frac{1}{r}v^2 = -\frac{1}{\rho}\frac{\partial p}{\partial r}+\upsilon\left(\frac{1}{r}\frac{\partial}{\partial r}\left(r\frac{\partial u}{\partial r}\right)+\frac{1}{r^2}\frac{\partial^2 u}{\partial \varphi^2}+\frac{\partial^2 u}{\partial z^2}-\frac{u}{r^2}+\frac{2}{r^2}\frac{\partial v}{\partial \varphi}\right) -\frac{\sigma B_0^2}{\rho}u \tag{2}$$

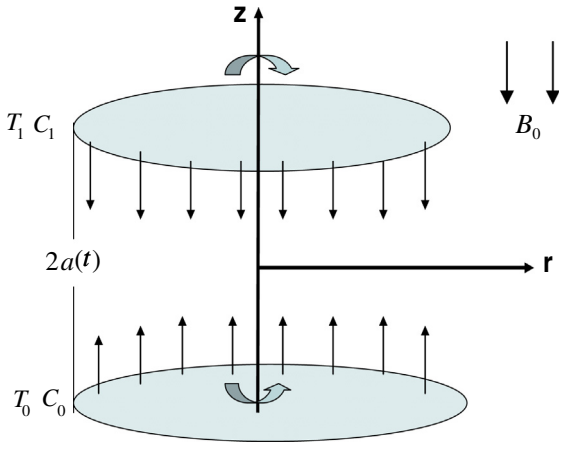

Figure 1 The model for expanding or contracting porous disks.

$$\frac{\partial v}{\partial t}+u\frac{\partial v}{\partial r}+\frac{1}{r}v\frac{\partial v}{\partial \varphi}+w\frac{\partial v}{\partial z}-\frac{1}{r}vu = -\frac{1}{\rho r}\frac{\partial p}{\partial \varphi}+\upsilon\left(\frac{1}{r}\frac{\partial}{\partial r}\left(r\frac{\partial v}{\partial r}\right)+\frac{1}{r^2}\frac{\partial^2 v}{\partial \varphi^2}+\frac{\partial^2 v}{\partial z^2}-\frac{v}{r^2}-\frac{2}{r^2}\frac{\partial u}{\partial \varphi}\right) -\frac{\sigma B_0^2}{\rho}v \tag{3}$$

$$\frac{\partial w}{\partial t}+u\frac{\partial w}{\partial r}+\frac{1}{r}v\frac{\partial w}{\partial \varphi}+w\frac{\partial w}{\partial z} = -\frac{1}{\rho}\frac{\partial p}{\partial z}+\upsilon\left(\frac{1}{r}\frac{\partial}{\partial r}\left(r\frac{\partial w}{\partial r}\right)+\frac{1}{r^2}\frac{\partial^2 w}{\partial \varphi^2}+\frac{\partial^2 w}{\partial z^2}\right) \tag{4}$$

$$\frac{\partial T}{\partial t}+u\frac{\partial T}{\partial r}+\frac{1}{r}v\frac{\partial T}{\partial \varphi}+w\frac{\partial T}{\partial z} = \frac{\kappa}{\rho c_p}\left(\frac{1}{r}\frac{\partial}{\partial r}\left(r\frac{\partial T}{\partial r}\right)+\frac{1}{r^2}\frac{\partial^2 T}{\partial \varphi^2}+\frac{\partial^2 T}{\partial z^2}\right)+\frac{\mu}{\rho c_p}\Phi +\frac{Dk_T}{c_s c_p}\left(\frac{1}{r}\frac{\partial}{\partial r}\left(r\frac{\partial C}{\partial r}\right)+\frac{1}{r^2}\frac{\partial^2 C}{\partial \varphi^2}+\frac{\partial^2 C}{\partial z^2}\right) \tag{5}$$

$$\frac{\partial C}{\partial t}+u\frac{\partial C}{\partial r}+\frac{1}{r}v\frac{\partial C}{\partial \varphi}+w\frac{\partial C}{\partial z} = D\left(\frac{1}{r}\frac{\partial}{\partial r}\left(r\frac{\partial C}{\partial r}\right)+\frac{1}{r^2}\frac{\partial^2 C}{\partial \varphi^2}+\frac{\partial^2 C}{\partial z^2}\right) +\frac{Dk_T}{T_m}\left(\frac{1}{r}\frac{\partial}{\partial r}\left(r\frac{\partial T}{\partial r}\right)+\frac{1}{r^2}\frac{\partial^2 T}{\partial \varphi^2}+\frac{\partial^2 T}{\partial z^2}\right) \tag{6}$$

where u, v, and w are the components of velocity along r, φ, z directions respectively, ρ is the density, p is dimensional pressure, t is time, υ is kinematic viscosity, σ is electrical conductivity, B_0 is the strength of applied magnetic field, c_p is specific heat at constant pressure, κ is thermal conductivity, D is the coefficient of mass diffusivity, T_m is the mean temperature, k_T is thermal-diffusion ratio, c_s is concentration susceptibility, T and C are temperature and concentration of the fluid and $\Phi=\left(\frac{\partial u}{\partial z}\right)^2+\left(\frac{\partial v}{\partial z}\right)^2$. The boundary conditions are the no-slip condition and no-temperature jump condition at the lower and upper disks [5,6]:

$$u=0,\quad v=Sr\Omega,\quad w=v_w=A\dot{a},\quad T=T_1,\quad C=C_1 \text{ at } z=a(t) \tag{7}$$

$$u=0,\quad v=r\Omega,\quad w=-sv_w=-A_0\dot{a},\quad T=T_0,\quad C=C_0 \text{ at } z=-a(t) \tag{8}$$

where Ω is the angular velocity of the lower disk, $S\Omega$ is the angular velocity of the upper disk, T_1 and C_1 are temperature and concentration at the upper disk, T_0 and C_0 are temperature and concentration at the lower disk, $A_0=sA$ is the coefficient of injection or suction which is the measure of disk permeability. Note that when $s=1$ the disks have equal permeability. $S=-1$ represents the case where the rotation velocity is same for both the disks.

By considering the similarity transformations like Von Kármán [1] for the velocity components, temperature and concentration in such a way that satisfies continuity eq. (1) identically.

$$u=\frac{-\upsilon r}{2a^2}F'(\eta),\quad w=\frac{2\upsilon}{a}F(\eta),\quad v=\frac{\upsilon r}{a^2}G(\eta),\quad T=T_0+(T_1-T_0)\theta(\eta),\quad C=C_0+(C_1-C_0)\phi(\eta),\quad \eta=\frac{z+a}{2a} \tag{9}$$

Eliminating pressure in Eqs. (2) and (4) and substituting Eq. (9) into Eqs. (2)–(6) and then by following Xinhui et al. [6], one obtains the following system of nonlinear differential equations

$$f^{IV}+\alpha(12f''-2f'''+4\eta f''')-4Rff'''-16\frac{R^{*2}}{R}gg'-4M^2f'''=0 \tag{10}$$

$$g''+\alpha(8g-2g'+4\eta g')+4Rgf'-4Rfg'-4M^2g=0 \tag{11}$$

$$\theta''-2\alpha\mathrm{Pr}(\theta'-2\eta\theta')-4\mathrm{Pr}Rf\theta'+Ec\mathrm{Pr}\left(\frac{R^2f''^2}{4}+R^{*2}g'^2\right)+Du\mathrm{Pr}\phi''=0 \tag{12}$$

$$\phi''-2\alpha Sc(\phi'-2\eta\phi')-4ScRf\phi'+SrSc\theta''=0 \tag{13}$$

where $\alpha(t)=a\dot{a}/\upsilon$ is t and is defined to be positive for expansion and negative for contraction, $R=av_w/\upsilon=A_0\alpha=As\alpha$ is the permeation Reynolds number and is positive for injection and negative for suction, $R^*=\frac{a^2\Omega}{\upsilon}$ is the rotation Reynolds number, $M=\frac{\sqrt{\sigma}B_0a}{\sqrt{\mu}}$ is the Hartmann number and μ is the dynamic viscosity, $\mathrm{Pr}=\frac{\mu c_p}{\kappa}$ is the Prandtl number, $Ec=\frac{r^2\Omega^2}{c_p(T_1-T_0)}$ is the Eckert number, $Sc=\upsilon/D$ is the Schmidt number, $Sr=\frac{Dk_T(T_1-T_0)}{T_m\upsilon(C_1-C_0)}$ is the Soret number and $Du=\frac{Dk_T(C_1-C_0)}{c_sc_p\upsilon(T_1-T_0)}$ is the Dufour number and prime(s) denote differentiation with respect to η. The corresponding boundary conditions are

$$f'(1)=0,\quad f(1)=\frac{1}{2},\quad g(1)=S,\quad \theta(1)=1,\quad \phi(1)=1 \tag{14}$$

$$f'(0)=0,\quad f(0)=\frac{-1}{2}s,\quad g(0)=1,\quad \theta(0)=0,\quad \phi(0)=0 \tag{15}$$

2.1. Solution of the problem

In this section, we give the analytical approximation to Eqs. (10)–(13) with the boundary conditions (14) and (15). For HAM solutions of Eqs. (10)–(13), the initial approximations f_0, g_0, θ_0 and ϕ_0 and the auxiliary linear operators L_1, L_2, L_3 and L_4 are as follows

$$f_0(\eta)=-(s+1)\eta^3+\frac{3}{2}(s+1)\eta^2-\frac{s}{2},\quad g_0=(S-1)\eta+1,\quad \theta_0=\eta,\quad \phi_0=\eta \tag{16}$$

$$L_1(f)=\frac{d^4f}{d\eta^4},\quad L_2(g)=\frac{d^2g}{d\eta^2},\quad L_3(\theta)=\frac{d^2\theta}{d\eta^2},\quad L_4(\phi)=\frac{d^2\phi}{d\eta^2} \tag{17}$$

with $L_1(c_1\eta^3+c_2\eta^2+c_3\eta+c_4)=0$, $L_2(c_5\eta+c_6)=0$, $L_3(c_7\eta+c_8)=0$, and $L_4(c_9\eta+c_{10})=0$ where $c_i(i=1-10)$ are constants. We refer the reader [5,13,17–20] for further details on HAM.

2.2. Convergence of HAM solution

The convergence of HAM solutions depends on the convergence control parameter h [16]. If h is chosen properly the homotopy series solution may converge fast. We find the region of convergence for the analytical solutions by plotting h-curves in Fig. 2 at 20th order approximation as suggested by Liao [16]. It is clear from Fig. 2 that the region of convergence for admissible values of h is $-0.2 \leqslant h \leqslant -0.61$. Later we show that the HAM solutions are of good agreement with numerical solutions.

3. Results and discussion

In this section, the graphical results are displayed to understand the effects of various pertinent parameters on the dimensionless temperature and concentration distributions through the Figs. 3–9 by considering $h = -0.4$, as proper value. We justify the proper choice of h by comparing HAM solutions and numerical solutions. Fig. 3 illustrates the temperature distribution, for different values of Pr, for the hydrodynamic case in the absence of viscous dissipation and mass diffusion. It is observed that for the symmetric condition, the temperature profiles are asymmetric about $\eta = 0.5$ and the profiles become flatter near the center region between the disks. The temperature boundary layer decreases with an increase of Pr as noted by Xinhui et al. [6]. Fig. 4 elucidates the effect of rotational Reynolds number on the dimensionless temperature distribution. Fig. 4a and b are plotted to see the effect of R^* on θ for the case of viscous dissipation with hydromagnetic effects. It is clear that θ is an increasing function of R^*. Fig. 4c corresponds to the flow between stationary impermeable disks for the case of hydrodynamic flow in the absence of viscous dissipation. The temperature distribution exhibits an oscillatory character with a rise in R^*. A similar behavior of the temperature distribution is reported by Xinhui et al. [6] and Nazir and Mahmood [5]. Fig. 5a and b depicts the effect of Dufour number Du for various values of Eckert number Ec on the dimensionless temperature distribution θ. From these figures one can observe that θ is an increasing function of Du. Further, quantitatively, when $\eta = 0.5$ and Du raises from 0.2 to 0.4 and Ec from 0.05 to 0.2, it is observed that in the value of θ there is 78.39% increase for the case of expansion combined injection and 40.41% increase in the case of contraction combined injection. From Fig. 6a and b it is clear that θ increases for a given increase in the Soret number Sr.

Figs. 7–9 illustrate the variation in the dimensionless concentration field ϕ for different values of s, Du and Sr respectively. The effect of s on ϕ is shown in Fig. 7a and b. It is noticed that ϕ is a decreasing function of s for the both cases of expansion and contraction combined with suction. Fig. 8a and b elucidates the effect of Dufour number Du for various values of Eckert number Ec on the dimensionless concentration distribution ϕ. From these figures one can observe that ϕ is a decreasing function of Du. Further, quantitatively, when $\eta = 0.5$ and Du increases from 0.2 to 0.4 and Ec increases from 0.05 to 0.2, there is 90.06% decrease in the value of ϕ for the case of expansion combined with injection and 43.24% decrease for the case of contraction combined with injection. Fig. 9a and b depicts the effect of Soret number Sr for various values of Eckert number Ec on the dimensionless concentration distribution ϕ. From these figures one can observe that ϕ decreases for a given increase in Sr and Ec. For instance, when $\eta = 0.5$ and Sr increases from 1 to 1.5 and Ec from 0.05 to 0.2, there is 123.79% decrease in the value of ϕ for the case of expansion combined with injection and 42.45% decrease for the case of contraction combined with injection. Therefore, the influence of thermal-diffusion and diffusion-thermo on the concentration field has a significant effect in the presence of viscous dissipation.

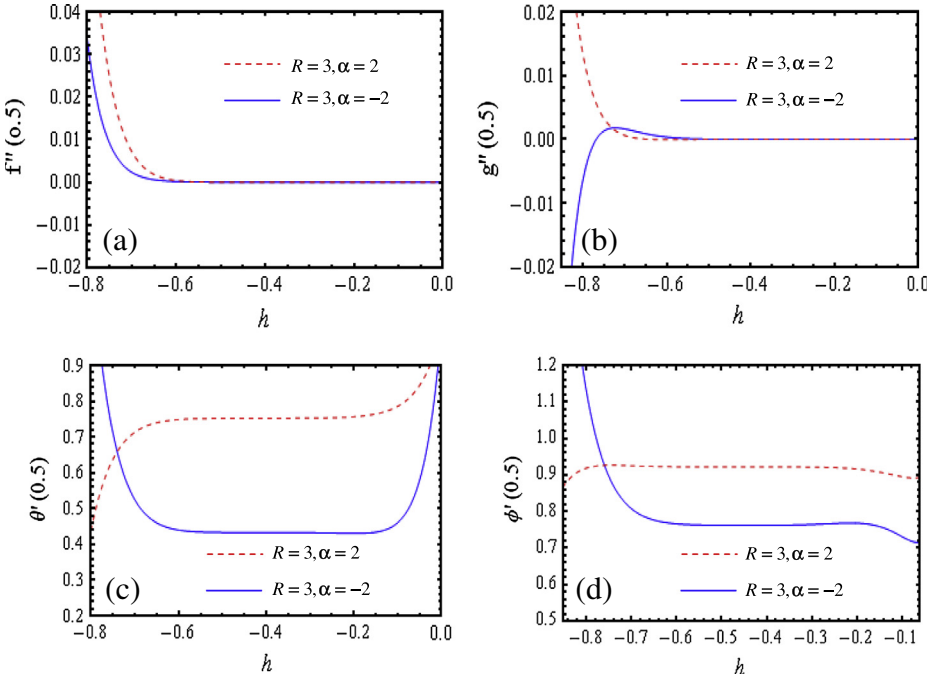

Figure 2 h-Curves for the 20th order approximations for the functions f, g, θ, ϕ for $s = 1$, $R^* = 0.5$, $M = 1$, $S = -1$, Pr = 0.71, $Ec = 0.2$, $Sc = 0.65$, $Sr = 1$, $Du = 0.03$.

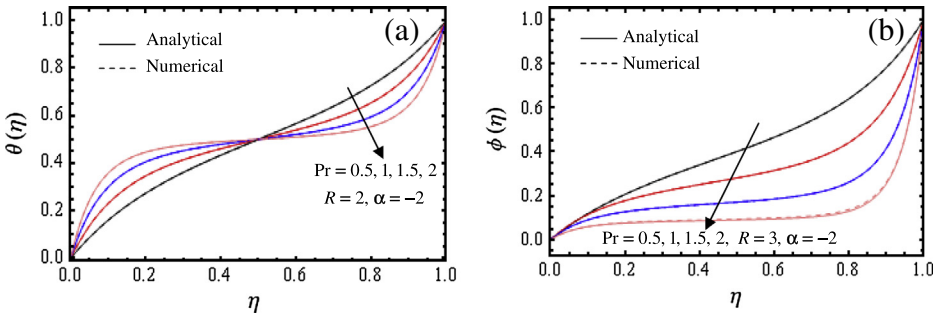

Figure 3 Effect of Pr on temperature distribution for, $Ec = 0$, $M = 0$, $Sc = 0$, $Sr = 0$, $Du = 0$. (a) $S = -1$, $s = 1$ $R^* = 0.5$, and (b) $S = -0.5$, $s = 0.5$, $R^* = 0.5$.

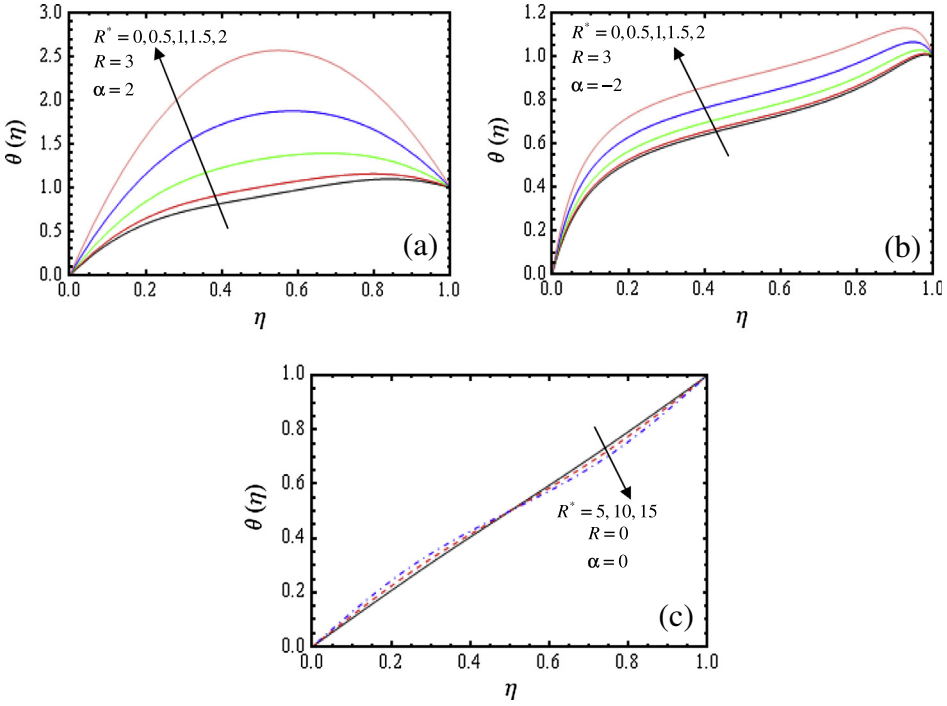

Figure 4 Effect of R^* on temperature distribution for (a) and (b) $s = 1$, Pr = 0.71, $M = 1$, $S = -1$, $Ec = 0.2$, $Sc = 0.65$, $Sr = 1$, $Du = 0.06$, and (c) $s = 1$, Pr = 0.7, $M = 0$, $S = -1$, $Ec = 0$, $Sc = 0.0$, $Sr = 0$, $Du = 0$.

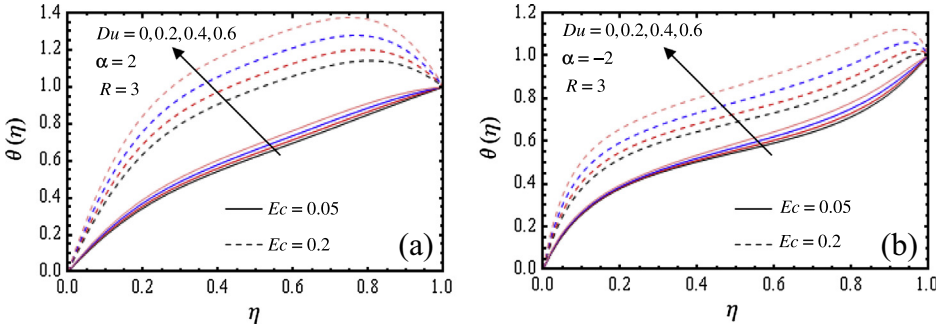

Figure 5 Effect of Du on temperature distribution for $s = 1$, $Ec = 0.2$, $M = 1$, $S = -1$, $R^* = 0.5$, $Sc = 0.65$, $Sr = 1$, Pr = 0.71.

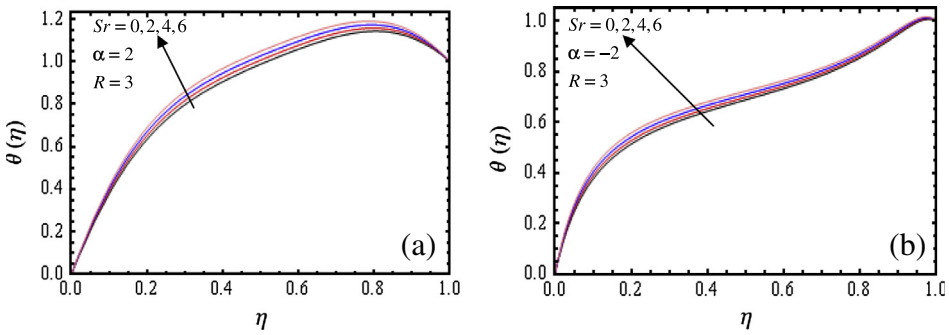

Figure 6 Effect of Sr on temperature distribution for $s = 1$, $Ec = 0.2$, $M = 1$, $S = -1$, $R^* = 0.5$, $Sc = 0.65$, $Du = 0.06$, Pr = 0.71.

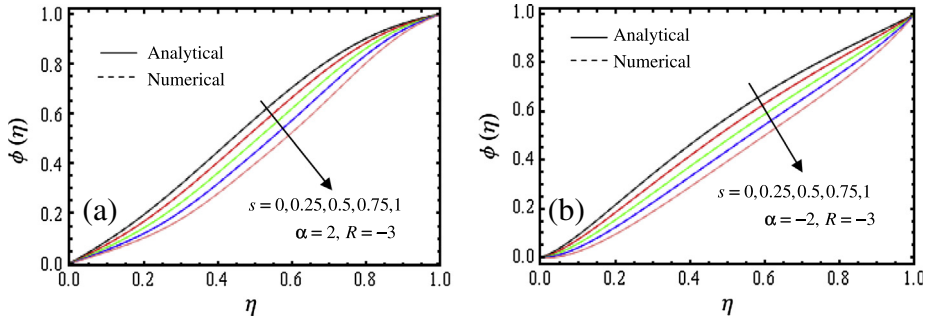

Figure 7 Effect of s on concentration distribution for $R^* = 0.5$, Pr = 0.71, $M = 1$, $S = -1$, $Ec = 0.2$, $Sc = 0.65$, $Sr = 1$, $Du = 0.06$.

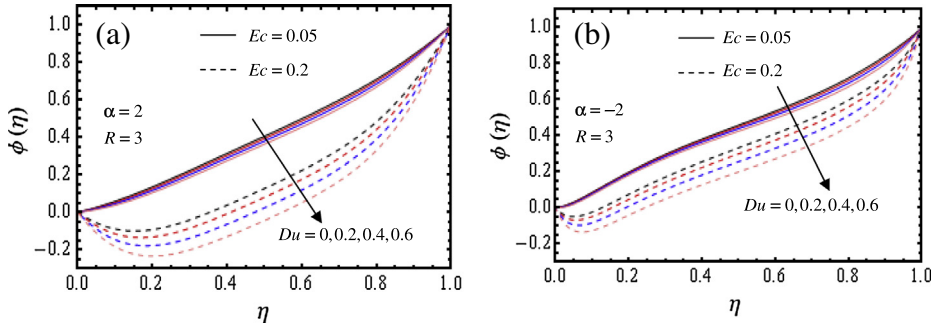

Figure 8 Effect of Du on concentration distribution for $s = 1$, $M = 1$, $S = -1$, $R^* = 0.5$, $Sc = 0.65$, $Sr = 1$, Pr = 0.71.

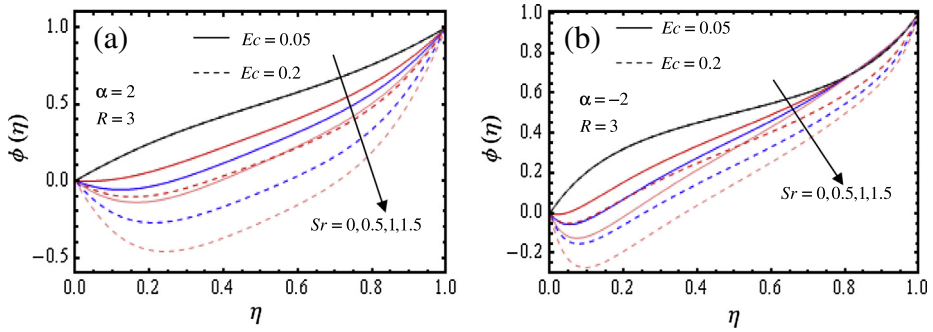

Figure 9 Effect of Sr on concentration distribution for $s = 1$, $Ec = 0.2$, $M = 1$, $S = -1$, $R^* = 0.5$, $Sc = 0.65$, $Du = 0.06$, Pr = 0.71.

Table 1 Numerical values of $f(\eta)$, $\theta(\eta)$ and ϕ (η) obtain by HAM (20th order) with convergence control parameter $h = -0.4$ and numerical Scheme when $\alpha = -2$, $R = -3$, $s = 0.5$, Pr = 0.71 $R^* = 0.5$, $M = 1$, $S = -1$, $Ec = 0.2$, $Sc = 0.65$, $Sr = 1$, $Du = 0.06$.

η	$f(\eta)$		$\theta(\eta)$		$\phi(\eta)$	
	Analytical	Numerical	Analytical	Numerical	Analytical	Numerical
0.0	−0.25	−0.25	0	0	0	0
0.1	−0.221097	−0.221097	0.223926	0.223943	0.056757	0.056700
0.2	−0.152305	−0.152305	0.380125	0.380138	0.154476	0.154436
0.3	−0.061894	−0.061894	0.512274	0.512281	0.263758	0.263743
0.4	0.039032	0.039032	0.632077	0.632078	0.374818	0.374828
0.5	0.143182	0.143183	0.740837	0.740835	0.483954	0.483980
0.6	0.244986	0.244986	0.836738	0.836735	0.589494	0.589525
0.7	0.339126	0.339126	0.917088	0.917088	0.690832	0.690856
0.8	0.419317	0.419317	0.978054	0.978057	0.788902	0.788911
0.9	0.477057	0.477057	1.011950	1.01196	0.887946	0.887944
1.0	0.5	0.5	1	1	1	1

The HAM solutions for the nonlinear coupled ordinary differential Eqs. (10)–(13) along with conditions (14) and (15) have been compared with the numerical values obtained by using shooting method coupled with Runge–Kutta scheme for the dimensionless temperature and concentration distributions and are presented in Figs. 3 and 7. Further, the numerical values have been tabulated in Table 1 for axial velocity, temperature and concentration distributions. The numerical results presented in the graphical and tabular form show an excellent agreement between numerical and HAM solutions.

4. Conclusion

In this study we have examined the effects of thermal-diffusion and diffusion-thermo on MHD flow of viscous fluid between expanding or contracting rotating porous disks with viscous dissipation. The convergence of obtained series solutions is analyzed. The results obtained by HAM are in good agreement with numerical solutions obtained by shooting method coupled with Runge–Kutta scheme. The temperature distribution increases while the concentration decreases with an increase in R, R^*, Du, Sr. The corresponding results of the problem for the hydrodynamic case can be recovered as a limiting case of the present analysis by taking $M = 0$. The results of Xinhui et al. [6], in the absence of mass diffusion can be captured as a special case of our analysis by taking $M = 0$. The flow analysis of Nazir and Mahmood [5], which corresponds to the hydrodynamic flow between two impermeable disks, can be recovered as a special case of the present analysis by taking $R = 0$, $s = 1$, $M = 0$, $Ec = 0$, and $Du = 0$.

Acknowledgments

Authors are thankful to the referees for their constructive comments and suggestions. The author (SS) gratefully acknowledge NBHM, Government of India for sanctioning a project under the Grant No. 2/48(19)/2012/NBHM(R.P.)/R&D II/9137.

References

[1] T. Von Kármán, Uber laminare und turbulente Reibung, Z. Angew. Math. Mach. 1 (1921) 233–252.
[2] M. Ashraf, M.A. Kamal, K.S. Syed, Numerical investigations asymmetric flow of a micropolar fluid between porous disks, Acta. Mach. Sin. 25 (2009) 787–794.
[3] H.K. Kuiken, The effect of normal blowing on the flow near the rotating disk of finite extent, J. Fluid Mech. 47 (1971) 789–798.
[4] E.M. Sparrow, G.S. Beavers, L.Y. Hung, Flow about a porous-surfaced rotating disk, Int. J. Heat Mass Transf. 14 (1971) 993–996.
[5] A. Nazir, T. Mahmood, Analysis of flow and heat transfer of viscous fluid between contracting rotating disks, Appl. Math. Model. 35 (2011) 3154–3165.
[6] S. Xinhui, Z. Liancun, Z. Xinxin, S. Xinyi, Homotopy analysis method for the asymmetric laminar flow and heat transfer of viscous fluid between contracting rotating disks, Appl. Math. Model. 36 (2012) 1806–1820.
[7] S. Uchida, A. Aoki, Unsteady flows in a semi-infinite contracting or expanding pipe, J. Fluid Mech. 82 (1977) 371–381.
[8] J. Majdalani, C. Zhou, C.A. Dawson, Two-dimensional viscous flow between slowly expanding or contracting walls with week permeability, J. Biomech. 35 (2002) 1399–1403.
[9] J. Majdalani, C. Zhou, Moderate-to-large injection and suction driven channel flows with expanding or contracting walls, Z. Angew. Math. Mech. 83 (2003) 181–196.
[10] E.C. Dauenhauer, J. Majdalani, Unsteady flows in semi-infinite expanding channels with wall injection, AIAA Paper 99-3523, 1999.
[11] S. Xinhui, Z. Liancun, Z. Xinxin, Y. Jainhong, Homotopy analysis method for the heat transfer in a asymmetric porous channel with an expanding or contracting wall, Appl. Math. Model. 35 (2011) 4321–4329.
[12] A.J. Chamka, A. Ben-Nakhi, MHD mixed convection-radiation interaction along a permeable surface immersed in a porous medium in the presence of Soret and Dufour's effects, Heat Mass Transf. 44 (2008) 845–856.
[13] T. Hayat, M. Nawaz, S. Asghar, S. Mesloub, Thermal-diffusion and diffusion-thermo effects on axisymmetric flow of a second grade fluid, Int. J. Heat Mass Transf. 54 (2011) 3031–3041.
[14] E. Osalusi, J. Side, R. Harris, Thermal-diffusion and diffusion-thermo effects on combined heat and mass transfer of a steady hydromagnetic convective slip flow due to a rotating disk with viscous dissipation and ohmic heating, Int. Commun. Heat Mass Transf. 35 (2008) 908–915.
[15] S. Srinivas, A. Subramanyam Reddy, T.R. Ramamohan, A study on thermal-diffusion and diffusion-thermo effects in a two-dimensional viscous flow between slowly expanding or contracting walls with weak permeability, Int. J. Heat Mass Transf. 55 (2012) 3008–3020.

[16] S.J. Liao, Beyond Perturbation: Introduction to Homotopy Analysis Method, CRC Press, Chapman and Hall, Boca Raton, 2003.
[17] X. Hang, Z.L. Lin, S.J. Liao, J. Majdalani, Homotopy based solutions of the Navier–Stokes equations for a porous channel with orthogonally moving walls, Phys. Fluids 22 (2010) 053601–053618.
[18] S. Abbasbandy, The application of homotopy analysis method to nonlinear equations arising heat transfer, Phys. Lett. A 360 (2006) 109–113.
[19] S.J. Liao, An analytic solution of unsteady boundary-layer flows caused by an impulsively stretching plate, Commun. Nonlinear Sci. Numer. Simulat. 11 (2006) 326–339.
[20] S. Srinivas, A. Gupta, S. Gulati, A. Subramanyam Reddy, Flow and mass transfer effects on viscous fluid in a porous channel with moving/stationary walls in presence of chemical reaction, Int. Commun. Heat Mass Transf. 48 (2013) 34–39.